Communication

Identification of Mo-based Precipitates in Haynes 282 Superalloy

L.O. OSOBA, A.K. KHAN, and O.A. OJO

Electron microscopy analyses were used to unambiguously identify the crystallographic nature of the largely speculated about Mo-based and carbon-rich intergranular precipitates in a newer γ' precipitation strengthened nickel-based superalloy, Haynes 282.

DOI: 10.1007/s11661-017-3999-8

Precipitation-strengthened nickel-based superalloys are widely used for the fabrication of hot section components of aircraft and power generation gas turbine engines. The ever-increasing demand for superalloys that can operate at higher operating temperatures in gas turbines, for improved efficiency, has resulted in the development of a γ' precipitation strengthened nickel-based superalloy Haynes 282. The alloy was developed with chemistry modification to enable a unique combination of excellent creep properties and thermal stability that meet and surpass those of commonly used superalloys, such as Waspaloy, Inconel 718, HY 263, and Rene 41.[1] A key factor that influences creep properties and elevated temperature microstructural stability of superalloys is the nature of second phase precipitates that form along the grain boundaries of a superalloy. Therefore, to adequately understand the influence of microstructure on high temperature performance of the new superalloy Haynes 282, proper identification of the nature of the second phase precipitates that form along its intergranular regions after standard heat treatment is imperative. Previous study has showed that sub-micron particles including $M_{23}C_6$ and M_5B_3, which cannot be unambiguously identified by conventional scanning electron microscopy but rather requires the use of transmission electron microscopy, form on the grain boundaries of Haynes 282 superalloy.[2] In the present work, along with the $M_{23}C_6$ and M_5B_3, another set of sub-micron particles of a different phase from the $M_{23}C_6$ and M_5B_3 and rich in molybdenum are found along the grain boundaries of the alloy after standard heat treatment. Transmission electron microscopy identification of this Mo-rich phase is reported and discussed in this communication.

The Haynes 282 superalloy used in this study was provided by Haynes International Inc., Kokomo, Indiana, USA, in the form of mill bright-annealed plates of dimensions $610 \times 120 \times 11.5$ mm. The nominal chemical composition of the material (wt pct) is 1.5Al, 2.1Ti, 10Co, 20Cr, 8.5Mo, 1.5Fe, 0.3Mn, 0.15Si, 0.06C, 0.005B, and balance nickel. The as-received alloy was subjected to a recommended standard full heat treatment (SFHT) at 1393 K (1120 °C) for 2 hours and water-quenched followed by aging at 1283 K (1010 °C) for 2 hours and air-cooled + 1061 K (788 °C) for 8 hours and air-cooled. Metallographically prepared specimens of the alloy for scanning electron microscopy examination were chemically etched with the use of modified Kalling's reagent—40 mL distilled water + 480 mL HCl + 48 g of $CuCl_2$ and electrolytically etched in 10 pct Oxalic acid at 6V for 3 to 5 seconds. Microstructural study was performed using a JEOL 5900 scanning electron microscope (SEM), a FEI Tecnai F20 (scanning) transmission electron microscopy ((S)TEM), and a JEOL 2100F STEM. The two microscopes are equipped with Oxford energy dispersive spectrometer (EDS) and Tecnai F20 is equipped with X-Max Silicon Drift Detector. TEM specimens were prepared by mechanical grinding 3-mm-diameter disks to ~150 μm and then twin-jet electropolishing them in solution of 10 pct perchloric acid, 30 pct butanol, and 60 pct methanol at 243 K (−30 °C) and 25 V.

Microstructure of the SFHTed specimen is shown in Figure 1. The alloy contains MC carbides dispersed within the austenitic γ matrix phase. Fine sub-micron-sized precipitates were formed along the grain boundaries. The nature of the intergranular particles, which cannot be identified using the SEM because of the inherent limitation of the spatial resolution of the SEM-EDS to reliably analyze sub-micron particles, have been studied by TEM analyses by the present authors and reported elsewhere.[2] The particles were found to consist of Ti-based MC carbides, Cr-based $M_{23}C_6$ carbides, and Mo-based M_5B_3 borides.[2] Further TEM study of the superalloy Haynes 282, in the present work, revealed another type of intergranular Mo-based precipitates in the SFHT condition of the material. The Mo-based precipitates have a complex fcc crystallographic structure in contrast to the bct tetragonal crystal structure of the Mo-based M_5B_3 boride particles. TEM X-ray microanalysis of the Mo-based particles, in the present work, did not reveal distinct boron peak but instead shows a distinct carbon peak (Figure 2), which suggests the particles to be likely carbides. There are two main types of secondary carbides, $M_{23}C_6$ and M_6C, that can form during aging heat treatment at 1023 K to 1328 K (750 °C to 1055 °C) in nickel-based superalloys. The two carbide

L.O. OSOBA is with the Department of Metallurgical and Materials Engineering, University of Lagos, P. O. Box 223, Akoka, Lagos State, Nigeria. A.K. KHAN and O.A. OJO are with the Department of Mechanical Engineering, University of Manitoba, Winnipeg, MB R3T 5V6, Canada. Contact e-mail: olanrewaju.ojo@umanitoba.ca

Manuscript submitted October 8, 2016.
Article published online February 7, 2017

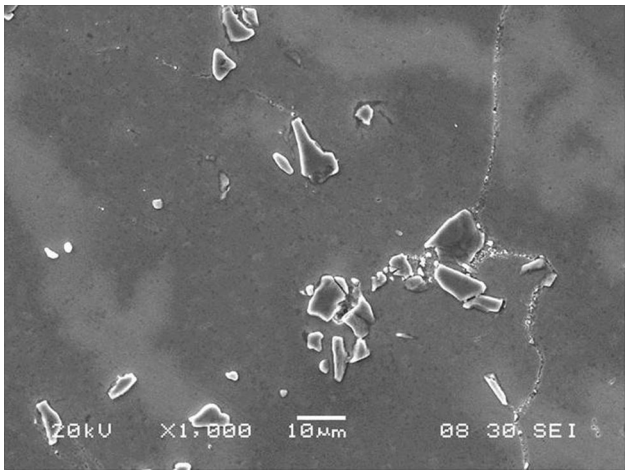

Fig. 1—Scanning electron micrograph of the standard full heat-treated Haynes 282 superalloy.

types have close crystallographic structure and, as such, it can be quite challenging to differentiate between the two carbides. They both have a complex fcc crystal structure and lattice parameter in the range of 1.06 to 1.12 nm. The inability to compute lattice parameter to a high level of precision, by the analysis of selected area diffraction pattern (SADP) in a TEM, makes it difficult to unambiguously differentiate between the two types of carbides. Nevertheless, systematic analyses of various diffraction patterns from different zone axes can be used to identify and confirm the nature of the carbides. In addition, Abdel-Latif *et al.*[3] have reported that due to the difference in the space groups of $M_{23}C_6$ and M_6C carbides, one way of distinguishing them is to examine their SADP obtained when their [001] zone axis is parallel to the electron beam. The inherent difference between the crystallographic structure factors of the two phases is such that while the kinematically forbidden {200} double reflections exists in the [001] zone axis SADP of $M_{23}C_6$ carbides, the {200} double reflections are absent in the

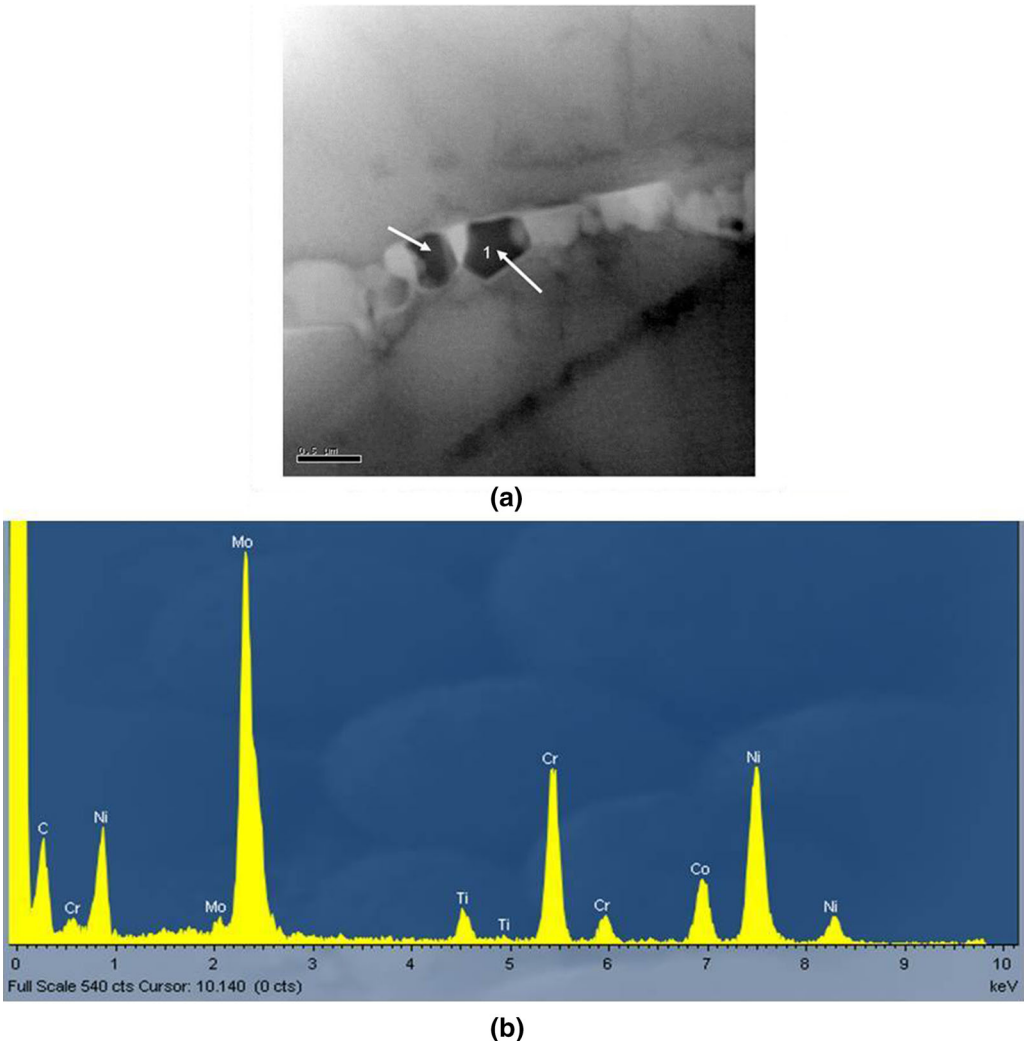

Fig. 2—(*a*) Transmission electron microscopy image of an intergranular Mo-based particle rich in carbon. (*b*) X-ray Energy Dispersive Spectroscopy Spectrum from the intergranular Mo-based particle rich in carbon.

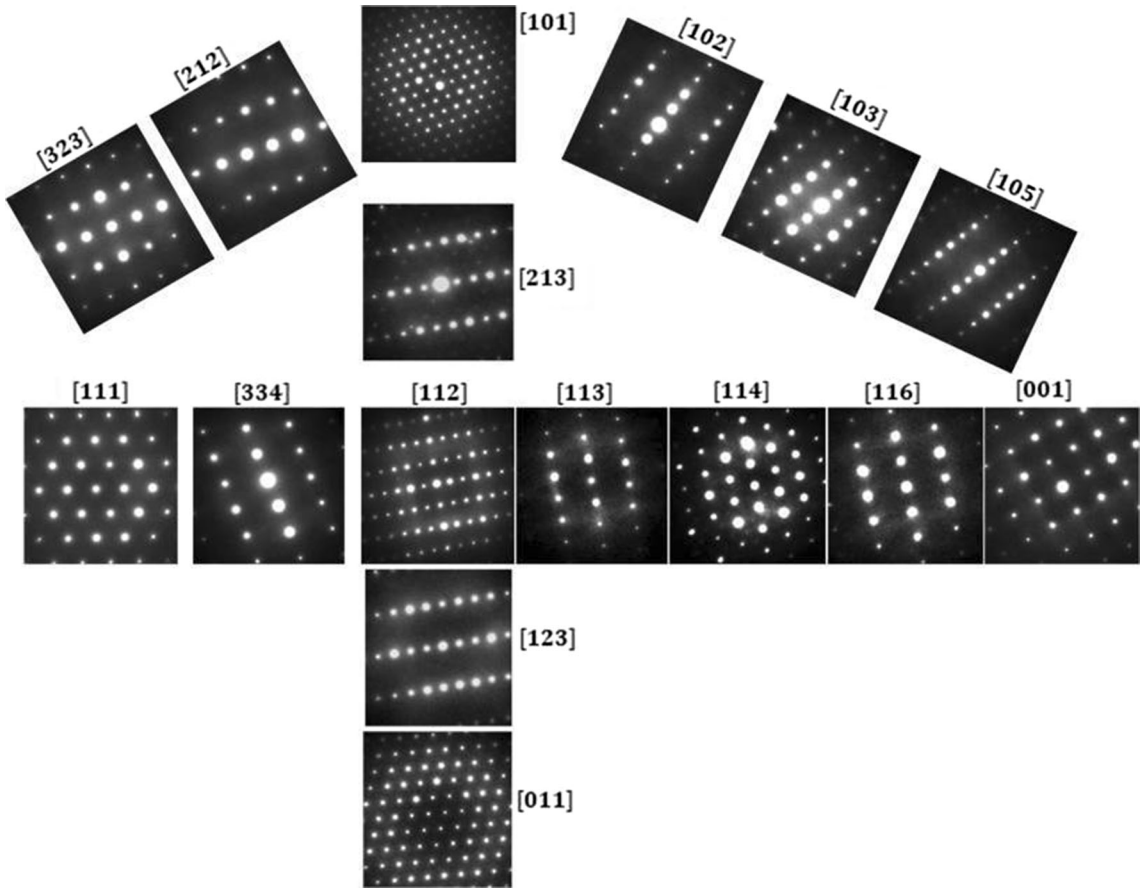

Fig. 3—Collage of selected area electron diffraction patterns from different zone axes of the M_6C carbide.

SADP from [001] zone axis in the M_6C carbides. In the present work, analyses of SADPs obtained by systematic tilting of the Mo-based particles that are free of boron to various zone axis, presented in Figure 3, shows that the particles are M_6C carbides with a lattice parameter of 1.12 nm. An indexed [001] zone axis SADP taken from the M_6C carbide is shown separately in Figure 4(a), and as seen from the Figure, the diffraction pattern is free of the kinematically forbidden {200} double reflections. Auxiliary confirmation of the crystallographic structure of the M_6C carbide phase was performed by convergent beam electron diffraction (CBED) analysis. The technique involves the use of a highly convergent beam of electrons to obtain diffraction information from a very small area (1 to 2 nm) in contrast to selected area diffraction where parallel beam is used to get the diffraction information from a comparatively much larger area. The CBED is used to determine the crystallographic point group and space group of a crystal based on the symmetries of CBED patterns obtained in close packed directions. Figure 4(b) is a CBED pattern in [111] zone axis that shows a 3m whole pattern symmetry. CBED patterns in Figure 4(c) and (d) show whole pattern symmetries of 4 and 2 mm, respectively, in [001] and [101] zone axes. According to the International Tables for Crystallography, m $\bar{3}$m point group is the only one that can give the diffraction symmetries in all the three zone axes observed in this work. The m $\bar{3}$m point group is consistent with the M_6C carbide identification. The positive identification of the M_6C carbide, enabled by the detailed TEM analyses performed in this work, addresses the long standing speculation on the nature of the Mo-based phase rich in carbon observed in wrought Haynes 282 superalloy.[4]

Boron is generally added to nickel-based superalloys to improve their resistance to creep rupture at elevated temperatures. The boron addition, however, could influence the structure and chemistry of grain boundary precipitates.[5,6] The solid solubility of boron in austenitic alloys is quite low, and it is reported that the maximum solubility of boron in 18 pct Cr to 15 pct Ni stainless steel at 1398 K (1125 °C) is 97 ppm of boron.[7] The solubility, however, decreases rapidly with decreasing temperature and becoming less than 30 ppm at 1173 K (900 °C) . Moreover, the size of boron atom is larger than the common interstitial elements in nickel (*e.g.*, C) and smaller than substitutional elements like Co and Cr. The size misfit of boron atoms in both the substitutional and interstitial sites in austenitic lattice implies that it would be energetically favorable for boron atoms to segregate to loosely packed regions like grain boundaries and other incoherent phase boundaries. Interfacial segregation of boron has been experimentally observed in a number of superalloys and austenitic alloys.[8–10] It has been, however, found that during intergranular segregation, boron tend to have stronger affinity for partitioning into second phase

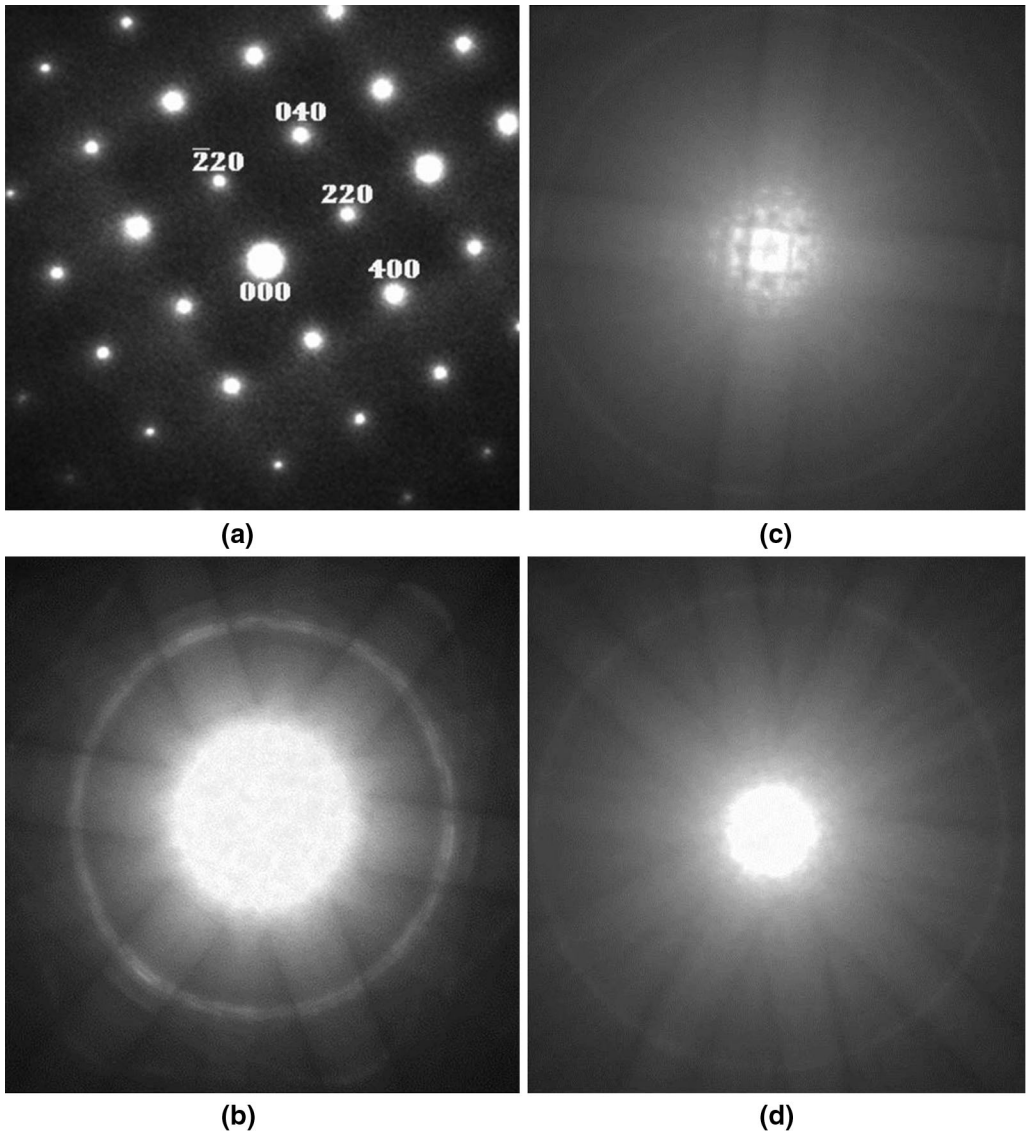

Fig. 4—(*a*) Selected area electron diffraction pattern obtained from [001] zone axis of the M_6C carbide, (*b* through *d*) Convergent electron diffraction patterns from [111], [001], and [101] zone axes, respectively, showing 3 m, 4 mm, and 2 mm whole pattern symmetry.

particles rather than remaining in solid solution form on grain boundaries.[6,8–12] Therefore, this may explain why aside from the Mo-based M_6C carbides, intergranular particles in the SFHT condition of the Haynes 282 superalloy also contain Mo-based M_5B_3 boride particles, as previously reported by the present authors.[2]

The authors gratefully acknowledge financial support from NSERC of Canada and Material donation by Haynes International Inc.

REFERENCES

1. L.M. Pike: in *TMS (The Minerals, Metals & Materials Society)*, R.C. Reed, K.A. Green, C. Pierre, T.P. Gabb, M.G. Fahrmann, E.S. Huron, and S.A. Woodard, eds., 2008, pp. 191–200.
2. L.O. Osoba, R.G. Ding, and O.A. Ojo: *Metall. Mater. Trans. A*, 2012, vol. 43A, pp. 4281–95.
3. A.M. Abdel-Latif, J.M. Corbett, and D.M.R. Taplin: *Met. Sci.*, 1982, vol. 16, pp. 199–206.
4. C.J. Boehlert and S.C. Longanbach: *Mater. Sci. Eng. A*, 2011, vol. 528, pp. 4888–98.
5. D.H. Maxwell, J.F. Baldwin, and J.F. Radavich: Metall. Met. Forming, 1975, p. 332.
6. M. Kurban, U. Erb, and K.T. Aust: *Scr. Mater.*, 2006, vol. 54, pp. 1053–58.
7. H.J. Goldschmidt: *J. Iron Steel Inst.*, 1971, vol. 209, p. 910.
8. X. Huang, M.C. Chaturvedi, N.L. Richards, and J. Jackman: *Acta Mater.*, 1997, vol. 45, p. 3095.
9. H. Guo, M.C. Chaturvedi, N.L. Richards, and G.S. McMahon: *Scr. Mater.*, 1999, vol. 40, p. 383.
10. W. Chen, M.C. Chaturvedi, and N.L. Richards: *Metall. Trans. A*, 2001, vol. 32A, p. 931.
11. O.A. Idowu, O.A. Ojo, and M.C. Chartuverdi: *Mater. Weld. J.*, 2009, vol. 88, pp. 179s–87s.
12. H.R. Zang, O.A. Ojo, and M.C. Chartuverdi: *Scr. Mater.*, 2008, vol. 58, pp. 167–70.